Hindawi Publishing Corporation
Advances in Physical Chemistry
Volume 2011, Article ID 584082, 9 pages
doi:10.1155/2011/584082

Research Article

Suppression of Intramolecular Vibrational Energy Redistribution by Intense CW-Laser Fields

M. Sugawara

Department of Fundamental Science and Technology, Graduate School of Science and Technology, Keio University, 3-14-1 Hiyoshi, Kohoku-ku, Yokohama 223-8522, Japan

Correspondence should be addressed to M. Sugawara, michi@chem.keio.ac.jp

Received 18 January 2011; Revised 5 April 2011; Accepted 26 May 2011

Academic Editor: Joel Bowman

We present a quantum control scheme which realizes suppression of the intramolecular vibrational energy redistribution (IVR). In this scheme, we utilize effective decomposition brought by intense CW-laser fields, which enables to exclude the doorway state coupled to background manifolds. In doing so, we introduce a helper state and make it optically coupled with the doorway state through the intense CW-laser field. We have applied the present scheme to both the Bixon-Jortner model and the $SCCl_2$ model system.

1. Introduction

In coherent laser control of molecular vibrations, the key feature is manipulation of vibrational coherence. Thus, dissipative processes such as dephasing and population decay have been considered as formidable obstacles. One of the typical dissipative processes is intramolecular vibrational energy redistribution (IVR), which is characterized as irreversible population flow from the doorway state to the background manifolds [1–5]. There have been several attempts to suppress the IVR by laser irradiation. For example, the suppression of IVR is theoretically confirmed under a strong resonant CW-laser excitation, in which total population is trapped on the initial and doorway states, and it rapidly oscillates between those two states [6]. It is also reported that the IVR can be restricted by the laser field, in which the frequency is swept [7, 8]. This phenomena is explained by the concept of adiabatic passages and the population is locked on the doorway state during the chirp pulse. In those approaches, only the suppression of IVR is considered, and there is no concept of controlling the population dynamics which escape from the IVR. Thus, it is necessary to apply additional control fields if one aims to drive the system to a specific desired quantum state while avoiding the IVR. However, additional laser would interfere with those existing "population locking" or "IVR-suppression" fields.

Another possible approach towards the suppression of IVR is to design the control field which actively manipulate phase relations between the eigenstates contained in the current wave packet. This could be done by optimal control theory (OCT) or local control theory (LCT) [9–13]. However, optimized laser fields tend to show complicated and highly sensitive nature since they try to control numerous eigenstates with various eigenenergies, which makes difficult to prepare the control laser in practice.

The main purpose of this study is to propose an alternative control scheme applicable to dissipative systems with which one can overcome the difficulties stated above. The basic idea is very simple. First, we effectively decompose the total system into target space and its complimentary space as we have shown in our former studies [14, 15]. By doing this, we can exclude the doorway state which is responsible for the dissipative dynamics, or IVR, from the system of interest, while remaining indirect optical transitions for control process. Furthermore, choosing a small space consisting of a few states as a target space, one can apply the well-established control schemes such as π-pulse [16] or stimulated Raman adiabatic passage (STIRAP) [17], which greatly simplifies the control process. The mechanism

of exclusion of the doorway state is well investigated for the 3-level system, in which two lasers are applied with static detuning [18]. The decomposition mechanism we adopt in the present work is basically the same as the one in [18] except the fact that the detuning itself is introduced as the induced Stark shift. We discuss the difference of those two approaches and clarify the advantageous features of the present scheme from a viewpoint of applicability to quantum control.

As a model system, we employ the classic IVR model system, Bixon-Jortner(BJ) model [19], to confirm the effectiveness of the present method and show how the IVR process can be excluded from the molecular system dynamics. Next, as an example of more realistic system, we choose $SCCl_2$ molecule, whose IVR is well studied, and there exists reliable model Hamiltonian [20, 21].

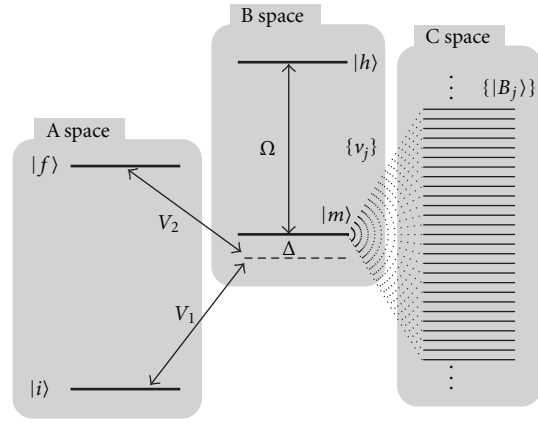

Figure 1: Schematic energy level diagram of a general IVR model system together with definitions of A, B and C spaces.

2. Theoretical

In the present work, we consider a model system as shown in Figure 1. Before proceeding to the formulation, we explain several terms used. Here, $|i\rangle$ is the initial state, which is typically taken to be the lowest vibrational state on the ground electronic state. The state $|m\rangle$ is the intermediate state, which optically connects the two states $|i\rangle$ and $|f\rangle$. The state $|f\rangle$ is the control target state, that is, we aim to transfer the initial population to $|f\rangle$ avoiding the population loss due to IVR process. Note that $|m\rangle$ is optically accessible from $|i\rangle$, $|f\rangle$, and $|h\rangle$ and also coupled with $\{|B_j\rangle\}$ $(j = 1, 2, \ldots, M)$ through the intramolecular interactions $\{v_j\}$. The IVR, that is, the irreversible population flow to $\{|B_j\rangle\}$, occurs through $|m\rangle$, thus, we call this state "doorway state", hereafter. In addition to that, we introduce the special state $|h\rangle$ which we call "helper state" in order to suppress the IVR process. This state is coupled through the intense CW-laser resonant to the transition between $|h\rangle$ and $|m\rangle$ with interaction strength Ω.

Next, we formally split the total system into three spaces as the follows. Control target space, which we call A space, consists of two states, initial $|i\rangle$ and final state $|f\rangle$. We define B space as the one spanned by a doorway state $|m\rangle$ and a helper state $|h\rangle$, which we utilize for realizing effective decomposition. C-space is defined as the space spanned by IVR background manifolds $\{B_j\}$.

The total Hamiltonian matrix under the rotating wave approximation (RWA) is given as

$$\begin{aligned}\mathbf{H} &= \mathbf{H}_0 + \lambda \mathbf{H}' \\ &\equiv \begin{pmatrix} \mathbf{\Delta_A} & \mathbf{0} & \mathbf{0} \\ \mathbf{0} & \mathbf{W_B} & \mathbf{0} \\ \mathbf{0} & \mathbf{0} & \mathbf{F_C} \end{pmatrix} + \lambda \begin{pmatrix} \mathbf{0} & \mathbf{V_{AB}} & \mathbf{0} \\ \mathbf{V_{BA}} & \mathbf{0} & \mathbf{V_{BC}} \\ \mathbf{0} & \mathbf{V_{CB}} & \mathbf{0} \end{pmatrix}.\end{aligned} \tag{1}$$

Here, we introduce the parameter λ so as to clearly specify the perturbation order. The optical interactions between $|i\rangle$ and $|m\rangle$ (V_1), and $|m\rangle$ and $|f\rangle$ (V_2) are taken to be much smaller than Ω. Minor matrices in (1) are defined as

$$\mathbf{\Delta_A} = \begin{pmatrix} \Delta & 0 \\ 0 & \Delta \end{pmatrix}, \qquad \mathbf{W_B} = \begin{pmatrix} \Omega & 0 \\ 0 & -\Omega \end{pmatrix},$$

$$\mathbf{F_C} = \begin{pmatrix} \epsilon_1 & 0 & 0 & 0 \\ 0 & \epsilon_2 & 0 & 0 \\ 0 & 0 & \ddots & 0 \\ 0 & 0 & 0 & \epsilon_M \end{pmatrix}, \tag{2}$$

where Δ denotes the detuning introduced for AB transition (see Figure 1), while $\{\epsilon_i\}$ $(i = 1, 2, \ldots, M)$ denotes the eigenenergies of the background manifolds in C-space. Note that we prediagonalize the B space Hamiltonian so as to make $\mathbf{W_B}$ diagonal matrix. The matrices $\mathbf{V_{AB}}$ (2×2) and $\mathbf{V_{BC}}$ $(2 \times M)$ correspond to the optical and static interactions, respectively.

The Schrödinger equation in the matrix representation is given as

$$\mathbf{H} \cdot \mathbf{U} = \mathbf{U} \cdot \mathbf{E}, \tag{3}$$

where $\mathbf{E}$ is a diagonal matrix with eigenvalues $\{E_i\}$ $(i = 1, 2, \ldots, N)$ in its diagonal elements, and $\mathbf{U}$ is the unitary matrix consisting of corresponding eigenvectors c_i $(i = 1, 2, \ldots, N)$ as $\mathbf{U} \equiv (\mathbf{c}_1, \mathbf{c}_2, \ldots, \mathbf{c}_N)$. Here, we expand $\mathbf{U}$ and $\mathbf{E}$ as

$$\begin{aligned}\mathbf{U} &= \mathbf{U}^{(0)} + \lambda \mathbf{U}^{(1)} + \lambda^2 \mathbf{U}^{(2)} + \cdots, \\ \mathbf{E} &= \mathbf{E}^{(0)} + \lambda \mathbf{E}^{(1)} + \lambda^2 \mathbf{E}^{(2)} + \cdots,\end{aligned} \tag{4}$$

where

$$\mathbf{U}^{(n)} = \begin{pmatrix} \mathbf{U}_{\mathbf{AA}}^{(n)} & \mathbf{U}_{\mathbf{AB}}^{(n)} & \mathbf{U}_{\mathbf{AC}}^{(n)} \\ \mathbf{U}_{\mathbf{BA}}^{(n)} & \mathbf{U}_{\mathbf{BB}}^{(n)} & \mathbf{U}_{\mathbf{BC}}^{(n)} \\ \mathbf{U}_{\mathbf{CA}}^{(n)} & \mathbf{U}_{\mathbf{CB}}^{(n)} & \mathbf{U}_{\mathbf{CC}}^{(n)} \end{pmatrix}, \qquad \mathbf{E}^{(n)} = \begin{pmatrix} \mathbf{E}_{\mathbf{A}}^{(n)} & \mathbf{0} & \mathbf{0} \\ \mathbf{0} & \mathbf{E}_{\mathbf{B}}^{(n)} & \mathbf{0} \\ \mathbf{0} & \mathbf{0} & \mathbf{E}_{\mathbf{C}}^{(n)} \end{pmatrix}. \tag{5}$$

Here, $\mathbf{E}_{\mathbf{A}}^{(n)}$, $\mathbf{E}_{\mathbf{B}}^{(n)}$, and $\mathbf{E}_{\mathbf{C}}^{(n)}$ are diagonal matrices, whose diagonal elements are nth perturbation energies. Inserting (1), (4) into (3) and comparing λ^n $(n = 0, 1, 2)$ terms gives the followings:

$$\mathbf{H}_0 \cdot \mathbf{U}^{(0)} = \mathbf{U}^{(0)} \cdot \mathbf{E}^{(0)}, \tag{6}$$

$$\mathbf{H}_0 \cdot \mathbf{U}^{(1)} - \mathbf{U}^{(1)} \cdot \mathbf{E}^{(0)} + \mathbf{H}' \cdot \mathbf{U}^{(0)} = \mathbf{U}^{(0)} \cdot \mathbf{E}^{(1)}, \tag{7}$$

$$\mathbf{H}_0 \cdot \mathbf{U}^{(2)} - \mathbf{U}^{(2)} \cdot \mathbf{E}^{(0)} - \mathbf{U}^{(1)} \cdot \mathbf{E}^{(1)} + \mathbf{H}' \cdot \mathbf{U}^{(1)} = \mathbf{U}^{(0)} \cdot \mathbf{E}^{(2)}. \tag{8}$$

From (6), one obtains the following equations for minor matrices:

$$\mathbf{\Delta}_{\mathrm{A}} \cdot \mathbf{U}_{\mathbf{AA}}^{(0)} = \mathbf{U}_{\mathbf{AA}}^{(0)} \cdot \mathbf{E}_{\mathbf{A}}^{(0)}, \tag{9}$$

$$\mathbf{W}_{\mathbf{B}} \cdot \mathbf{U}_{\mathbf{BB}}^{(0)} = \mathbf{U}_{\mathbf{BB}}^{(0)} \cdot \mathbf{E}_{\mathbf{B}}^{(0)}, \tag{10}$$

$$\mathbf{F}_{\mathbf{C}} \cdot \mathbf{U}_{\mathbf{CC}}^{(0)} = \mathbf{U}_{\mathbf{CC}}^{(0)} \cdot \mathbf{E}_{\mathbf{C}}^{(0)}, \tag{11}$$

while off-diagonal blocks of $\mathbf{U}^{(0)}$ are all zero matrices. As $\mathbf{\Delta}_{\mathbf{A}}$ commutes with $\mathbf{U}_{\mathbf{AA}}^{(0)}$, (9) gives $\mathbf{E}_{\mathbf{A}}^{(0)} = \mathbf{\Delta}_{\mathbf{A}}$, which leaves $\mathbf{U}_{\mathbf{AA}}^{(0)}$ undetermined. On the other hand, from (10), (11) one obtains that $\mathbf{U}_{\mathbf{BB}}^{(0)}$ and $\mathbf{U}_{\mathbf{CC}}^{(0)}$ are both determined as identity matrices of 2×2 and an $M \times M$, respectively, whereas $\mathbf{E}_{\mathbf{B}} = \mathbf{W}_{\mathbf{B}}$ and $\mathbf{E}_{\mathbf{C}} = \mathbf{F}_{\mathbf{C}}$. The first two terms of the left hand side of (7) are given as

$$\mathbf{H}_0 \cdot \mathbf{U}^{(1)} - \mathbf{U}^{(1)} \cdot \mathbf{E}^{(0)} = \begin{pmatrix} \mathbf{0} & \mathbf{\Delta}_{\mathbf{A}} \cdot \mathbf{U}_{\mathbf{AB}}^{(1)} - \mathbf{U}_{\mathbf{AB}}^{(1)} \cdot \mathbf{W}_{\mathbf{B}} & \mathbf{\Delta}_{\mathbf{A}} \cdot \mathbf{U}_{\mathbf{BC}}^{(1)} - \mathbf{U}_{\mathbf{BC}}^{(1)} \cdot \mathbf{F}_{\mathbf{C}} \\ \mathbf{W}_{\mathbf{B}} \cdot \mathbf{U}_{\mathbf{BA}}^{(1)} - \mathbf{U}_{\mathbf{BA}}^{(1)} \cdot \mathbf{\Delta}_{\mathbf{A}} & \mathbf{W}_{\mathbf{B}} \cdot \mathbf{U}_{\mathbf{BB}}^{(1)} - \mathbf{U}_{\mathbf{BB}}^{(1)} \cdot \mathbf{W}_{\mathbf{B}} & \mathbf{W}_{\mathbf{B}} \cdot \mathbf{U}_{\mathbf{BC}}^{(1)} - \mathbf{U}_{\mathbf{BC}}^{(1)} \cdot \mathbf{F}_{\mathbf{C}} \\ \mathbf{F}_{\mathbf{C}} \cdot \mathbf{U}_{\mathbf{CA}}^{(1)} - \mathbf{U}_{\mathbf{CA}}^{(1)} \cdot \mathbf{\Delta}_{\mathbf{A}} & \mathbf{F}_{\mathbf{C}} \cdot \mathbf{U}_{\mathbf{CB}}^{(1)} - \mathbf{U}_{\mathbf{CB}}^{(1)} \cdot \mathbf{W}_{\mathbf{B}} & \mathbf{F}_{\mathbf{C}} \cdot \mathbf{U}_{\mathbf{CC}}^{(1)} - \mathbf{U}_{\mathbf{CC}}^{(1)} \cdot \mathbf{F}_{\mathbf{C}} \end{pmatrix}, \tag{12}$$

whereas other terms are

$$\mathbf{H}' \cdot \mathbf{U}^{(0)} = \begin{pmatrix} \mathbf{0} & \mathbf{V}_{\mathbf{AB}} \cdot \mathbf{U}_{\mathbf{BB}} & \mathbf{0} \\ \mathbf{V}_{\mathbf{BA}} \cdot \mathbf{U}_{\mathbf{AA}}^{(0)} & \mathbf{0} & \mathbf{V}_{\mathbf{BC}} \cdot \mathbf{U}_{\mathbf{CC}} \\ \mathbf{0} & \mathbf{V}_{\mathbf{CB}} \cdot \mathbf{U}_{\mathbf{BB}} & \mathbf{0} \end{pmatrix},$$
$$\mathbf{U}_{\mathbf{AA}}^{(0)} \cdot \mathbf{E}_{\mathbf{AA}}^{(1)} = \begin{pmatrix} \mathbf{U}_{\mathbf{AA}}^{(0)} \cdot \mathbf{E}_{\mathbf{AA}}^{(1)} & \mathbf{0} & \mathbf{0} \\ \mathbf{0} & \mathbf{U}_{\mathbf{BB}}^{(0)} \cdot \mathbf{E}_{\mathbf{BB}}^{(1)} & \mathbf{0} \\ \mathbf{0} & \mathbf{0} & \mathbf{U}_{\mathbf{CC}}^{(0)} \cdot \mathbf{E}_{\mathbf{CC}}^{(1)} \end{pmatrix}. \tag{13}$$

Comparing the component of A space, one obtains the equation $\mathbf{U}_{\mathbf{AA}}^{(0)} \cdot \mathbf{E}_{\mathbf{AA}}^{(1)} = \mathbf{0}$, which leads to $\mathbf{E}_{\mathbf{AA}}^{(1)} = \mathbf{0}$ since $\mathbf{U}_{\mathbf{AA}}^{(0)}$ is a unitary matrix. Thus, there is no first-order correction onto the A space eigenenergies.

Next, comparing the BA-block of both sides of (7) leads to the equation

$$\mathbf{W}_{\mathbf{B}} \cdot \mathbf{U}_{\mathbf{BA}}^{(1)} - \mathbf{U}_{\mathbf{BA}}^{(1)} \cdot \mathbf{\Delta}_{\mathbf{A}} + \mathbf{V}_{\mathbf{BA}} \cdot \mathbf{U}_{\mathbf{AA}}^{(0)} = \mathbf{0}. \tag{14}$$

Considering $\mathbf{U}_{\mathbf{BA}}^{(1)} \cdot \mathbf{\Delta}_{\mathbf{A}} = \mathbf{\Delta}_{\mathbf{B}} \cdot \mathbf{U}_{\mathbf{BA}}^{(1)}$, (14) can be rewritten as

$$(\mathbf{W}_{\mathbf{B}} - \mathbf{\Delta}_{\mathbf{B}}) \cdot \mathbf{U}_{\mathbf{BA}}^{(1)} = -\mathbf{V}_{\mathbf{BA}} \cdot \mathbf{U}_{\mathbf{AA}}^{(0)}, \tag{15}$$

which leads to

$$\mathbf{U}_{\mathbf{BA}}^{(1)} = -(\mathbf{W}_{\mathbf{B}} - \mathbf{\Delta}_{\mathbf{B}})^{-1} \cdot \mathbf{V}_{\mathbf{BA}} \cdot \mathbf{U}_{\mathbf{AA}}^{(0)}. \tag{16}$$

Here, $\mathbf{\Delta}_{\mathbf{B}}$ denotes the identity matrix of B space multiplied by Δ. The prefactor matrix $(\mathbf{W}_{\mathbf{B}} - \mathbf{\Delta}_{\mathbf{B}})^{-1}$ in (16) is given in a simple form as

$$(\mathbf{W}_{\mathbf{B}} - \mathbf{\Delta}_{\mathbf{B}})^{-1} = \begin{pmatrix} \dfrac{1}{\Omega - \Delta} & 0 \\ 0 & \dfrac{1}{-\Omega - \Delta} \end{pmatrix}. \tag{17}$$

Note that $\mathbf{U}_{\mathbf{BA}}$ becomes zero matrix as Ω becomes large or $\Omega \gg \Delta$, which leads to the suppression of AB-space mixing.

Comparing CA-block of (7), one obtains

$$\mathbf{F}_{\mathbf{C}} \cdot \mathbf{U}_{\mathbf{CA}}^{(1)} - \mathbf{U}_{\mathbf{CA}}^{(1)} \cdot \mathbf{\Delta}_{\mathbf{A}} = \mathbf{0}, \tag{18}$$

which is rewritten as

$$(\mathbf{F}_{\mathbf{C}} - \mathbf{\Delta}_{\mathbf{C}}) \cdot \mathbf{U}_{\mathbf{CA}}^{(1)} = \mathbf{0}, \tag{19}$$

where $\mathbf{\Delta}_{\mathbf{C}}$ is $M \times M$ identity matrix multiplied by Δ. It is readily seen that $\mathbf{U}_{\mathbf{CA}}^{(1)} = 0$ since $\mathbf{F}_{\mathbf{C}} - \mathbf{\Delta}_{\mathbf{C}} \neq \mathbf{0}$. Thus, there is no first-order CA-mixing.

Next, we consider the second-order terms. With $\mathbf{E}^{(1)} = \mathbf{0}$, (8) becomes

$$\mathbf{H}_0 \cdot \mathbf{U}^{(2)} - \mathbf{U}^{(2)} \cdot \mathbf{E}^{(0)} + \mathbf{H}' \cdot \mathbf{U}^{(1)} = \mathbf{U}^{(0)} \cdot \mathbf{E}^{(2)}. \tag{20}$$

Since we focus on the dynamics of A space, we extract AA-block of (20) as

$$\mathbf{\Delta_A}\cdot\mathbf{U}_{\mathbf{AA}}^{(2)}-\mathbf{U}_{\mathbf{AA}}^{(2)}\cdot\mathbf{\Delta_A}+\mathbf{V_{AB}}\cdot\mathbf{U}_{\mathbf{BA}}^{(1)}=\mathbf{U}_{\mathbf{AA}}^{(0)}\cdot\mathbf{E}_{\mathbf{A}}^{(2)}. \tag{21}$$

Considering that the first two terms of (21) are canceled out and inserting (16), one obtains

$$\mathbf{V_{AB}}\cdot(\mathbf{W_B}-\mathbf{\Delta_B})^{-1}\cdot\mathbf{V_{AB}}\cdot\mathbf{U}_{\mathbf{AA}}^{(0)}=\mathbf{U}_{\mathbf{AA}}^{(0)}\cdot\mathbf{E}_{\mathbf{A}}^{(2)}. \tag{22}$$

Note that (22) is an eigenvalue equation, which determines the second-order energy correction $\mathbf{E}_{\mathbf{A}}^{(2)}$ onto A space as well as corresponding eigenvectors $\mathbf{U}_{\mathbf{AA}}^{(0)}$. Here, we define the A space effective Hamiltonian $\mathbf{H}_{\mathbf{A}}^{(\mathrm{eff})}$ as

$$\mathbf{H}_{\mathbf{A}}^{(\mathrm{eff})}\equiv\mathbf{\Delta_A}+\mathbf{V_{AB}}\cdot(\mathbf{W_B}-\mathbf{\Delta_B})^{-1}\cdot\mathbf{V_{AB}}, \tag{23}$$

which determines the dynamics of A space within the second-order. Note that there is no interaction terms relevant to the C-space. This implies that as long as $\mathbf{H}'$ is relatively small enough and the second-order perturbation theory is applicable, the interactions between the doorway state and the background manifolds can be excluded from the system dynamics effectively.

Note that the perturbation expansion shown above is applied for the weak field V_i, which is responsible for interspace optical transitions. On the other hand, the strong interaction through CW-laser, which cannot be dealt with perturbation method, is precisely taken into account by prediagonalization of the B space.

Finally, we discuss possible side effect brought by optically allowed state $|m'\rangle$ adjacent to the intermediate state $|m\rangle$. Typically, the level spacing Δ' between $|m\rangle$ and $|m'\rangle$ is about $1000\,\mathrm{cm}^{-1}$. The CW-laser (Ω) applied for decomposition turns out to be off-resonant by Δ', which is large enough to exclude the undesired transition to $|m'\rangle$.

3. Results

To confirm the applicability of the present theory, we first apply it to well-known Bixon-Jortner model system [19]. In this model, all the background levels are equally spaced and coupled to a single bright doorway state $|m\rangle$ with uniform strength v. Shown in Figure 2(a) is the population dynamics under field-free condition while the initial state is taken to be $|m\rangle$. The coupling parameter v is taken to be 0.1Ω where as Ω denotes the unit frequency, which determines the timescale ($\sim\ \Omega^{-1}$) of the dynamics. It is shown that the irreversible population flow to the background manifolds $\{|B_j\rangle\}$ occurs due to the dephasing process between numerous eigenstates contained in the initial state $|m\rangle$.

Next, we try a naive population control in which control target is the population transfer from $|i\rangle$ to $|f\rangle$. We introduce two resonant CW-lasers corresponding to the transitions, $|i\rangle\ \leftrightarrow\ |m\rangle$, and $|m\rangle\ \leftrightarrow\ |f\rangle$, respectively. The total Hamiltonian corresponding to (1) is given as

$$\mathbf{H}=\begin{pmatrix}\Delta & 0 & V_1 & 0 & \cdots & 0\\ 0 & \Delta & V_2 & 0 & \cdots & 0\\ V_1 & V_2 & 0 & v & v & v\\ 0 & 0 & v & \epsilon_1 & \cdots & 0\\ \vdots & \vdots & v & \vdots & \epsilon_i & \vdots\\ 0 & 0 & v & 0 & \cdots & \epsilon_M\end{pmatrix}, \tag{24}$$

where the vertical and horizontal dots are all zeroes. Shown in Figure 2(b) is the population dynamics with the initial condition $|i\rangle$. Both optical interaction parameters V_1 and V_2 are taken to be $1.0\,\Omega$. As shown in Figure 2(b), significant amount of total population leaks to the background manifolds, and its nature is basically irreversible though coherent oscillations are observed in early-time stage. Note that such oscillatory nature of the population dynamics is rapidly damped, and the system finally settles into stationary state in which the population of $|f\rangle$ is only 25%. Thus, the control objective is hardly achieved with this approach.

Now, we introduce a helper state $|h\rangle$ in order to suppress the population loss due to IVR. The total Hamiltonian represented by the original basis set is given as

$$\widetilde{\mathbf{H}}=\begin{pmatrix}\Delta & 0 & V_1 & 0 & 0 & \cdots & 0\\ 0 & \Delta & V_2 & 0 & 0 & \cdots & 0\\ V_1 & V_2 & 0 & \Omega & v & v & v\\ 0 & 0 & \Omega & 0 & 0 & \cdots & 0\\ 0 & 0 & v & 0 & \epsilon_1 & \cdots & 0\\ \vdots & \vdots & v & \vdots & \vdots & \epsilon_i & \vdots\\ 0 & 0 & v & 0 & 0 & \cdots & \epsilon_M\end{pmatrix}, \tag{25}$$

where Ω is taken to be the optical interaction between $|m\rangle$ and $|h\rangle$ in this case. We reconstruct the basis set for B space so as to express the Hamiltonian matrix in the form of (2), that is,

$$\mathbf{H}=\begin{pmatrix}\Delta & 0 & V' & V' & 0 & \cdots & 0\\ 0 & \Delta & V'' & V'' & 0 & \cdots & 0\\ V' & V'' & \Omega & 0 & v' & v' & v'\\ V' & V'' & 0 & -\Omega & v' & v' & v'\\ 0 & 0 & v' & v' & \epsilon_1 & \cdots & 0\\ \vdots & \vdots & v' & v' & \vdots & \epsilon_i & \vdots\\ 0 & 0 & v' & v' & 0 & \cdots & \epsilon_M\end{pmatrix}, \tag{26}$$

where $V'=V_1/\sqrt{2}$, $V''=V_2/\sqrt{2}$, and $v''=v/\sqrt{2}$. Shown in Figure 2(c) is the population dynamics under the condition $V_1=V_2=0.01\,\Omega$. It is shown that the population oscillates between $|i\rangle$ and $|f\rangle$, and there is very little population leak into the background manifolds $\{|B_j\rangle\}$. This feature denotes

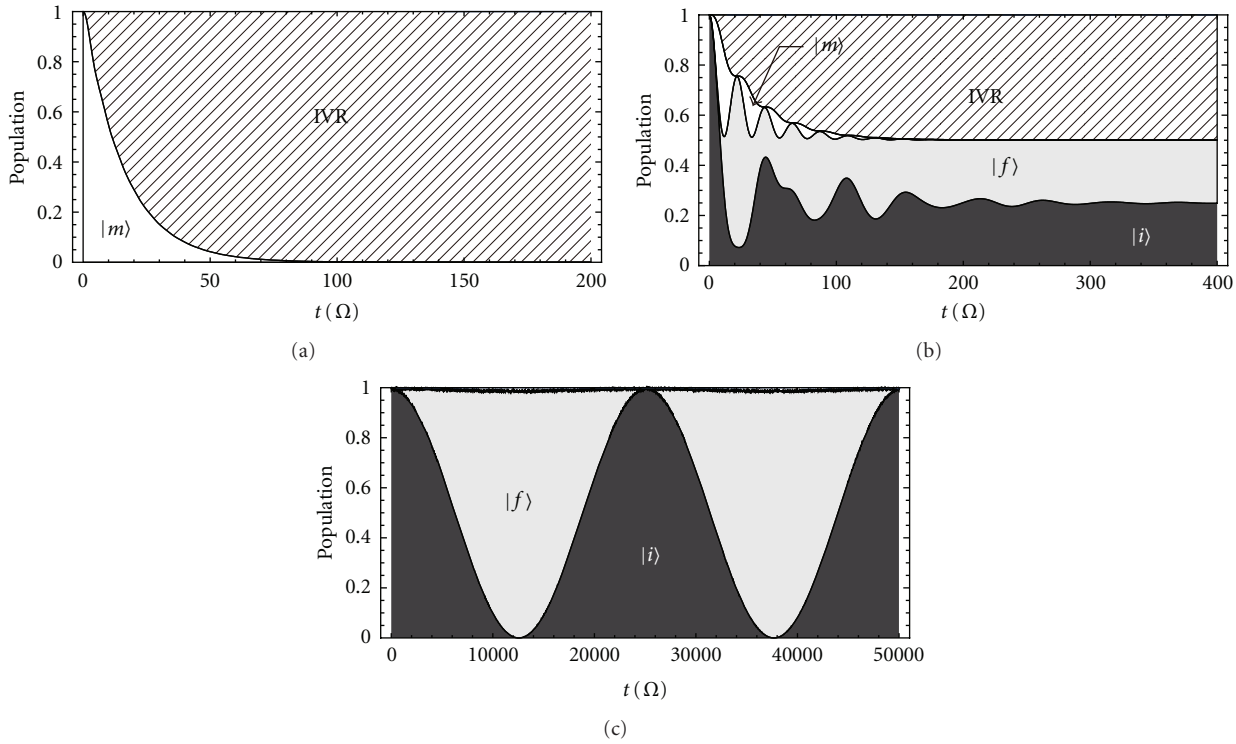

FIGURE 2: Population dynamics of Bixon-Jortner model. The dark gray, light gray, and white areas correspond to the population of $|i\rangle$, $|f\rangle$, and $|m\rangle$, respectively. The hatched area denoted by IVR corresponds to the population distributed over background manifolds $|B_j\rangle$. (a) $|m\rangle$ is taken to be the initial state. (b) Two CW-lasers, V_1 and V_2, are applied corresponding to the $|i\rangle$-$|m\rangle$ and $|m\rangle$-$|f\rangle$ transitions. Both V_1 and V_2 are taken to be 0.1 Ω. (c) Intense CW-laser is introduced to make the helper state $|h\rangle$ strongly coupled with $|m\rangle$ together with the relatively weak lasers V_1 and V_2.

that the control target space, that is, A space, is effectively isolated as a 2-level system without dissipative dynamics. The effective Hamiltonian for the A space can be obtained from (23) as

$$\mathbf{H}_{\mathbf{A}}^{(\mathrm{eff})} = \begin{pmatrix} \Delta & 0 \\ 0 & \Delta \end{pmatrix} + \frac{\Delta}{\Delta^2 - \Omega^2} \begin{pmatrix} V_1^2 & V_1 V_2 \\ V_2 V_1 & V_2^2 \end{pmatrix}. \tag{27}$$

It is clearly shown that the Rabi oscillation is driven by the second term which originates from the second-order interspace optical interaction between A and B spaces. Note also that this term is proportional to the detuning parameter Δ. This implies that common detuning is required for driving population dynamics in the A space.

As for a more realistic molecular system, we consider Thiophosgen ($SCCl_2$), which has six vibrational modes, and there exists IVR process among highly excited states. It is known that only a limited set of vibrational resonances are related to the dissipative dynamics, and an effective Hamiltonian consisting of six modes for describing the IVR process is proposed as [20]

$$\hat{H}_M = \hat{H}_M^{(0)} + \hat{H}_M', \tag{28}$$

where

$$\hat{H}_M^{(0)} = \sum_{i=1}^{6} \omega_i \left(n_i + \frac{1}{2} \right) + \sum_{i=1}^{6} \chi_{ii} \left(n_i + \frac{1}{2} \right)^2, \qquad \hat{H}_M' = V a^{3-\Delta n}. \tag{29}$$

Here $\Delta n = \sum_i |n_i - n_i'|$. We used the same parameters listed in [20]. As for the basis set, we take the direct product of the harmonic oscillator eigenfunctions with respect to each mode, which is denoted as $|n_1, n_2, n_3, n_4, n_5, n_6\rangle$. With RWA, the structure of the Hamiltonian matrix is essentially identical to (25). We consider the mode 1 (corresponding to CS-stretching motion) is optically allowed, and the bright doorway state is defined as $|8, 0, 0, 0, 0, 0\rangle$ as shown in Figure 3. The initial state $|i\rangle$ is taken to be the ground state $|0, 0, 0, 0, 0, 0\rangle$, and we aim to transfer the population onto the target final state $|f\rangle \equiv |12, 0, 0, 0, 0, 0\rangle$, which is one of the highly excited zero-order states of the CS-stretching mode with relatively long lifetime. The laser parameters are taken to be $V_1 = V_2 = 30\,\mathrm{cm}^{-1}$ and $\Delta = 30\,\mathrm{cm}^{-1}$. The corresponding laser amplitudes for V_1 and V_2 are estimated as $9.6 \times 10^9\,\mathrm{W/cm}^2$ and $5.0 \times 10^9\,\mathrm{W/cm}^2$, respectively [20].

Shown in Figure 4 are the population dynamics changing the CW-laser intensity Ω from $0\,\mathrm{cm}^{-1}$ to $300\,\mathrm{cm}^{-1}$. As shown in Figure 4(a), the irreversible population flow to the background modes 2–6, that is, IVR, occurs as we

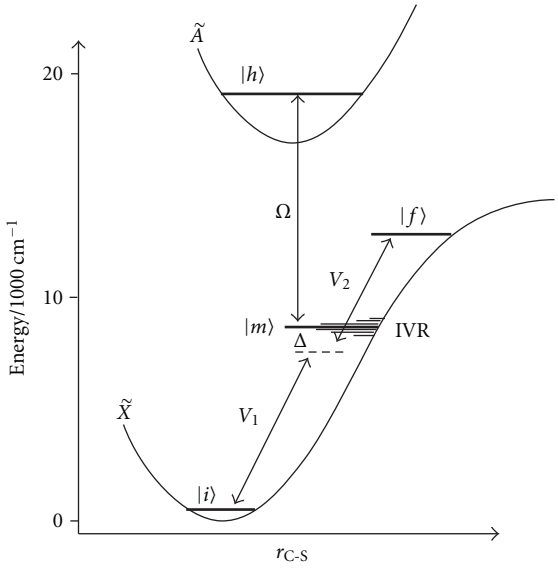

FIGURE 3: Schematic potential curve with energy levels for $SCCl_2$ molecule.

see in the Bixon-Jortner model case. As the laser power increases, the dissipative dynamics is gradually suppressed (see Figures 4(b), 4(c), and 4(d)) due to the decomposition effect, which isolates A space ($|i\rangle$ and $|f\rangle$). Finally, as shown in Figure 4(e), a neat Rabi oscillation appears in the population dynamics of A space, which implies that the target subspace can be effectively treated as a simple 2-level system. Then, one can apply conventional π-pulse scheme for population transfer onto $|f\rangle$ avoiding the population loss due to the IVR. Note also that the timescale of the Rabi oscillation in Figure 4(e) can be controlled by changing the detuning parameter Δ (see (27)).

Here, we should clearly state the difference in the decomposition conditions between the present method and the static detuning approach in [18]. In the present scheme, the detuning itself is introduced as the induced Stark shift, or a large energy splitting between the zero-order eigenvalues in B space, that is, $\pm\Omega$ in (2). Thus, the required condition for effective decomposition is different accordingly, that is, $\Delta \gg V_1, V_2$ in the static detuning case whereas $\Omega \gg \Delta$, $\Omega \gg V_1, V_2$, in the present method.

One of the important differences between those two schemes is the suppression efficiency with respect to the detuning value, Δ or Ω. To see this, we consider a simple 4-level system which consists of only A space ($|i\rangle$ and $|f\rangle$) and B space ($|m\rangle$ and $|h\rangle$). Instead of omitting C-space (background states), we introduce a phenomenological dephasing parameter γ associated with the intermediate state $|m\rangle$, that is, we introduce an imaginary component γ for the eigenvalue of $|m\rangle$. Here, we take $\gamma = 30\,\text{cm}^{-1}$ so as to reproduce the IVR timescale of $SCCl_2$. Shown in Figure 5(a) is the population dynamics with $\Omega = 0\,\text{cm}^{-1}$ and $V_1 = V_2 = 30\,\text{cm}^{-1}$, which corresponds to the condition of Figure 4(a). One can see that the dissipative IVR dynamics is qualitatively reproduced with the phenomenological parameter $\gamma = 30\,\text{cm}^{-1}$. The shown Figure 5(b) is the population dynamics with $\Omega = 300\,\text{cm}^{-1}$ corresponding to Figure 4(e), and the suppression effect works fine as expected. On the other hand, shown in Figure 5(c) is the result for static detuning case without using the helper state $|h\rangle$, that is, $\Omega = 0\,\text{cm}^{-1}$ and $\Delta = 300\,\text{cm}^{-1}$. As shown in the result, the suppression effect is insufficient compared to Figure 5(b), although the detuning is taken to be $300\,\text{cm}^{-1}$, in both cases. In order to achieve the suppression level of Figure 5(b), one needs to increase the detuning up to $\Delta = 3000\,\text{cm}^{-1}$ as shown in Figure 5(d). Thus, the static detuning approach requires ten times larger than that in the present case. In the practical application to $SCCl_2$, it is difficult to take required detuning $\Delta = 3000\,\text{cm}^{-1}$ because adjacent level exists within $1000\,\text{cm}^{-1}$.

Further investigation on the effective Hamiltonian clarifies the difference in suppression efficiency shown above. The effective Hamiltonian for the CW-laser-induced Stark shift detuning case is given as [15]

$$\mathbf{H}_{\mathbf{A}}^{(\text{eff})} = \begin{pmatrix} \Delta & 0 \\ 0 & \Delta \end{pmatrix} + \frac{\Delta}{(\Delta + i\gamma)\Delta - \Omega^2} \begin{pmatrix} V_1^2 & V_1 V_2 \\ V_2 V_1 & V_2^2 \end{pmatrix}, \quad (30)$$

whereas that of the static detuning case is [18]

$$\mathbf{H}_{\mathbf{A}}^{(\text{eff})} = \begin{pmatrix} \Delta & 0 \\ 0 & \Delta \end{pmatrix} + \frac{1}{\Delta + i\gamma} \begin{pmatrix} V_1^2 & V_1 V_2 \\ V_2 V_1 & V_2^2 \end{pmatrix}. \quad (31)$$

One can see that $\Delta \gg \gamma$ or $1 \gg (\gamma/\Delta)$ is required to neglect γ for static detuning case. On the other hand, the denominator of (30) shows that $1 \gg (\gamma\Delta/\Omega^2)$ is required. Note that the condition $1 \gg (\gamma\Delta/\Omega^2)$ can be satisfied with smaller (Stark shift) detuning because of its Ω^2 dependency. This is why ten times larger value ($\Delta = 3000\,\text{cm}^{-1}$) is needed in the static detuning approach in Figure 5(d). Note also that choosing small Δ helps to satisfy the exclusion of dissipation in the present method. Another difference is lying in the laser parameter dependence of the Rabi frequency driven by the effective Hamiltonian. In the static detuning approach, the control parameter Δ affects both decomposition condition and the time scale of the isolated system. On the other hand, in the present method, the decomposition condition is mainly determined by Ω, while the timescale of Rabi oscillation can be adjusted by changing Δ as far as $\Omega \gg \Delta$ stands. From a viewpoint of quantum control, the present approach may offer versatile control scheme because it has more handling parameters compared to the static detuning approach.

Apparent drawback of the present method is possible side effects induced by the intense CW-lasers, such as multiphoton transitions which eventually leads to ionization, or unexpected near-resonant transition. We, here, consider the limitation of the present method when it is applied to the realistic molecular system as shown above. Note that some results shown above are rather extreme cases. In practice,the $\Omega = 300\,\text{cm}^{-1}$ condition in Figure 4(e) corresponds to CW-laser intensity of $\sim 10^{11}\,\text{W/cm}^2$, which

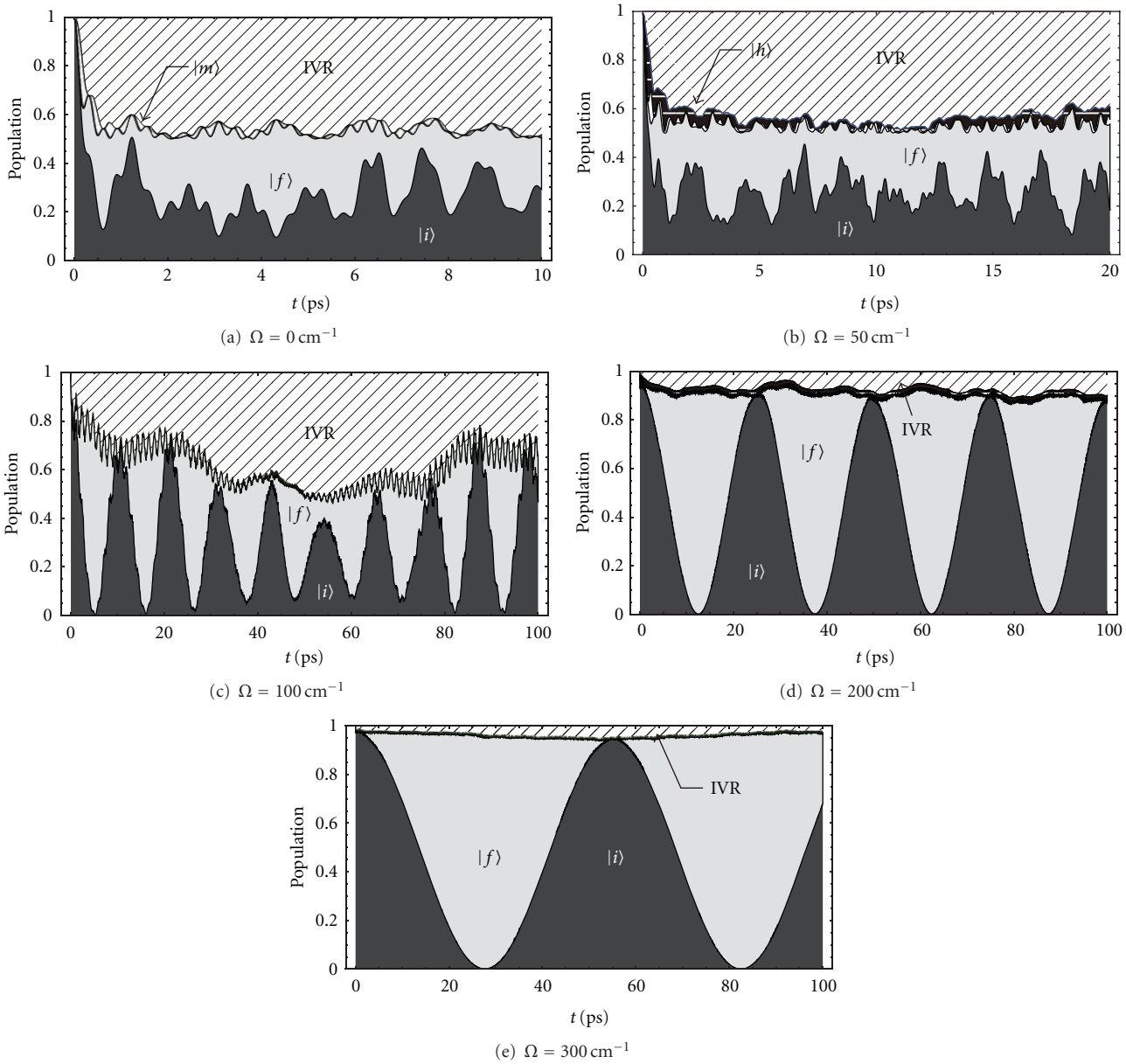

Figure 4: Population dynamics of $SCCl_2$ molecule with changing coupling parameter Ω. Corresponding laser power is as follows: (a) 0.0 W/cm^2, (b) 2.48×10^9 W/cm^2, (c) 9.91×10^9 W/cm^2, (d) 3.96×10^{10} W/cm^2, (e) 8.92×10^{10} W/cm^2. The hatched area denoted by IVR corresponds to the population distributed over background manifolds $|B_j\rangle$. The white area in (a) denotes the population of $|m\rangle$, whereas the area painted by black background with horizontal lines in (b) corresponds to the population of $|h\rangle$. Note that the population of $|m\rangle$ and $|h\rangle$ is so little and hardly seen in Figures 4(c) and 4(e).

may cause undesired resonant multiphoton excitation. However, milder condition, such as Figure 4(d) corresponding to $\sim 10^{10}$ W/cm^2 still works fairly well. Note also that the intensities of weak lasers for V_1 and V_2 can be taken lower than the decomposition field Ω by one order, which denotes that there are very few side processes caused by V_i interactions. Since resonant optical processes mainly occur under this condition, it could be possible to suppress undesired transitions by choosing helper level and laser frequency avoiding unexpected (near)resonances with care. Taking as large Δ value as possible also makes it possible to shorten the irradiation time of CW Laser, since we can expect faster Rabi-oscillation dynamics for control.

It is known that general IVR time scale varies from subpico to several hundreds ps [22]. For the IVR system with $\gamma \approx 10^0$ cm^{-1} $\sim 10^{-1}$ cm^{-1}, applicability of the present method becomes more plausible, because required CW-laser intensity turns out to be around 10^8 W/cm^2 $\sim$ 10^9 W/cm^2.

Finally, we should mention applicability of RWA for the present study. As the laser power increases, validity of RWA becomes doubtful. In order to verify this, we have carried out numerical calculation in which we treat the

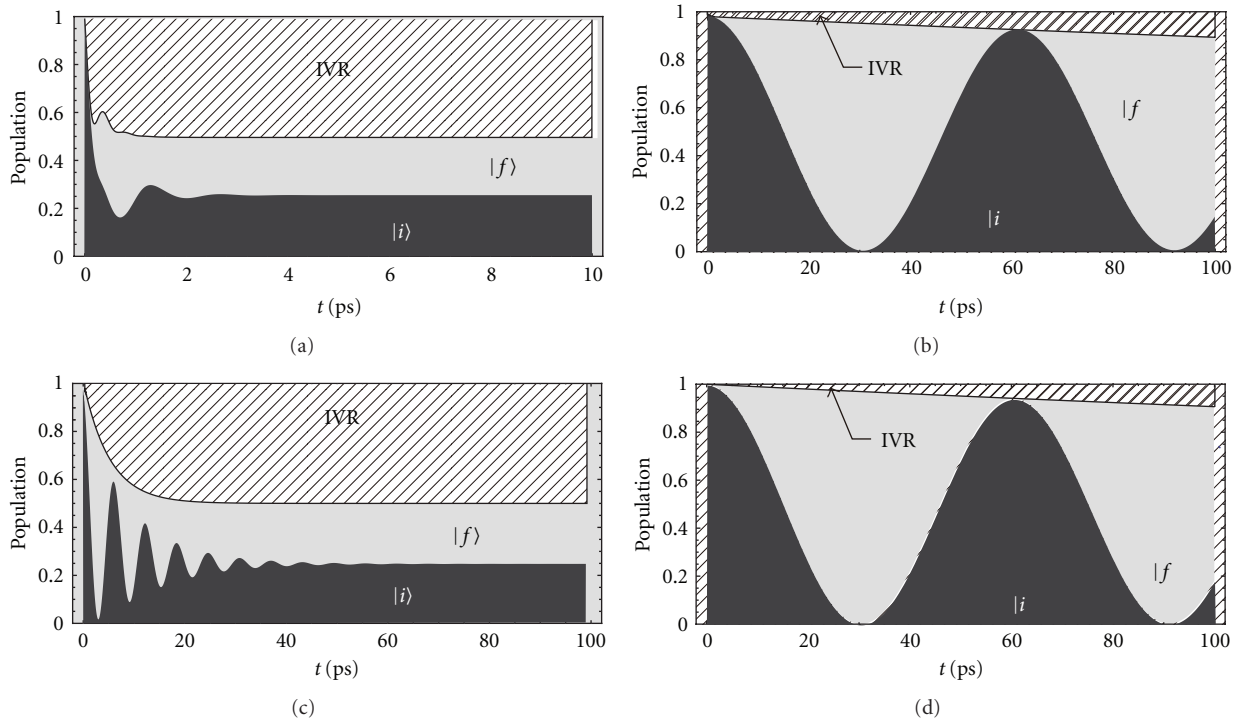

Figure 5: Comparison of suppression efficiency of Stark shift detuning (present method) and static detuning approaches. Shown in each figure is population dynamics of 4-level system with phenomenological dephasing parameter $\gamma = 30\,\text{cm}^{-1}$ on $|m\rangle$. V_1 and V_2 are taken to be $30\,\text{cm}^{-1}$. Other parameters are taken to be (a) $\Omega = 0\,\text{cm}^{-1}$, $\Delta = 30\,\text{cm}^{-1}$, (b) $\Omega = 300\,\text{cm}^{-1}$, $\Delta = 30\,\text{cm}^{-1}$, (c) $\Omega = 0\,\text{cm}^{-1}$, $\Delta = 300\,\text{cm}^{-1}$, and (d) $\Omega = 0\,\text{cm}^{-1}$, $\Delta = 3000\,\text{cm}^{-1}$.

laser fields semiclassically. Overall behaviors of population dynamics agree with the ones obtained with RWA. The only difference is additional high-frequency components with small amplitudes onto the Rabi oscillation in the semiclassical treatments. Thus, we have concluded that the RWA are appropriate approximation for the present work.

4. Summary

We have presented that the dissipative dynamics due to the dephasing, such as IVR, can be suppressed by utilizing the effective decomposition brought by the intense CW lasers. One of the unique features of the present scheme is that one can treat it within a time-independent picture with the help of RWA, which makes the problem easy to handle. Consequently, one can avoid the situation that the control laser fields becomes too complicated. Another intriguing feature is that one can control the time scale of the population dynamics by changing the detuning parameters and it can be taken even longer than that of IVR itself. This is quite advantageous feature from a viewpoint of control problem, because one can design the control field regardless of the time constant of the dissipation.

Acknowledgments

This paper was supported, in part, by the Japan Society for the Promotion of Science (JSPS), Grant-in-Aid for Scientific Research (C), KAKENHI (20550021).

References

[1] E. L. Sibert III and M. Gruebele, "Molecular vibrational energy flow and dilution factors in an anharmonic state space," *The Journal of Chemical Physics*, vol. 124, no. 2, Article ID 024317, 2006.

[2] S. Lee, M. Engel, and M. Gruebele, "The state space model of vibrational energy flow: An experimental test using SEP spectra of jet-cooled thiophosgene," *Chemical Physics Letters*, vol. 420, no. 1–3, pp. 151–156, 2006.

[3] M. Gruebele, "Mechanism and control of molecular energy flow: a modeling perspective," *Theoretical Chemistry Accounts*, vol. 109, no. 2, pp. 53–63, 2003.

[4] Y. Yamada, N. Mikami, and T. Ebata, "Real-time detection of doorway states in the intramolecular vibrational energy redistribution of the OH/OD stretch vibration of phenol," *Journal of Chemical Physics*, vol. 121, no. 23, article no. 5, pp. 11530–11534, 2004.

[5] I. Thanopulos, P. Brumer, and M. Shapiro, "Intramolecular energy transfer dynamics in 24-mode pyrazine by partitioning technique: a time-dependent approach," *Journal of Chemical Physics*, vol. 133, no. 15, Article ID 154111, 2010.

[6] S. Mukamel and K. Shan, "On the selective elimination of intramolecular vibrational redistribution using strong resonant laser fields," *Chemical Physics Letters*, vol. 117, no. 5, pp. 489–494, 1985.

[7] D. Goswami and W. Warren, "Control of chemical dynamics by restricting intramolecular vibrational relaxation," *The Journal of Chemical Physics*, vol. 99, no. 6, pp. 4509–4517, 1993.

[8] D. Goswami, "Multiphoton coherent control in complex systems," *Journal of Optics B*, vol. 7, no. 10, pp. S265–S269, 2005.

[9] Y. Ohtsuki, K. Nakagami, Y. Fujimura, W. Zhu, and H. Rabitz, "Quantum optimal control of multiple targets: development of a monotonically convergent algorithm and application to intramolecular vibrational energy redistribution control," *Journal of Chemical Physics*, vol. 114, no. 20, pp. 8867–8876, 2001.

[10] Y. Ohtsuki, G. Turinici, and H. Rabitz, "Generalized monotonically convergent algorithms for solving quantum optimal control problems," *Journal of Chemical Physics*, vol. 120, no. 12, pp. 5509–5517, 2004.

[11] S. Shi and H. Rabitz, "Quantum mechanical optimal control of physical observables in microsystems," *The Journal of Chemical Physics*, vol. 92, no. 1, pp. 364–376, 1990.

[12] H. Tang, R. Kosloff, and S. A. Rice, "A generalized approach to the control of the evolution of a molecular system," *Journal of Chemical Physics*, vol. 104, no. 14, pp. 5457–5471, 1996.

[13] M. Sugawara, "General formulation of locally designed coherent control theory for quantum system," *Journal of Chemical Physics*, vol. 118, no. 15, pp. 6784–6800, 2003.

[14] M. Sugawara, "A new quantum control scheme for multilevel systems based on effective decomposition by intense laser fields," *Journal of Chemical Physics*, vol. 130, no. 9, Article ID 094103, 2009.

[15] M. Sugawara, M. Tamaki, and S. Yabushita, "A new control scheme of multilevel quantum system based on effective decomposition by intense CW lasers," *Journal of Physical Chemistry A*, vol. 111, no. 38, pp. 9446–9453, 2007.

[16] P. Knight and P. Milonni, "The Rabi frequency in optical spectra," *Physics Report*, vol. 66, no. 2, pp. 21–107, 1980.

[17] K. Bergmann, H. Theuer, and B. Shore, "Coherent population transfer among quantum states of atoms and molecules," *Reviews of Modern Physics*, vol. 70, no. 3, pp. 1003–1025, 1998.

[18] D. Grischkowsky, M. M. T. Loy, and P. F. Liao, "Adiabatic following model for two-photon transitions: nonlinear mixing and pulse propagation," *Physical Review A*, vol. 12, no. 6, pp. 2514–2533, 1975.

[19] M. Bixon and J. Jortner, "Intramolecular radiationless transitions," *The Journal of Chemical Physics*, vol. 48, no. 2, pp. 715–726, 1968.

[20] R. Bigwood and M. Gruebele, "Freezing molecular vibrational energy flow with coherent control," *Journal of Molecular Structure: (THEOCHEM)*, vol. 589-590, pp. 447–457, 2002.

[21] R. Bigwood, B. Milam, and M. Gruebele, "The ground state vibrational structure of $SCCl_2$: observation of backbone IVR," *Chemical Physics Letters*, vol. 287, no. 3-4, pp. 333–341, 1998.

[22] D. J. Nesbitt and R. Field, "Vibrational energy flow in highly excited molecules: role of intramolecular vibrational redistribution," *Journal of Physical Chemistry*, vol. 100, no. 31, pp. 12735–12756, 1996.